Micropolar Fluid Flow over an Exponentially Stretching Curved Sheet with Variable Thermal Conductivity

By

Iqra Nasreen

RegistrationNo.:764-FBAS/MSMA/F21

Department of Mathematics & Statistics
Faculty of Sciences
International Islamic University, Islamabad
Pakistan
2024

Micropolar Fluid Flow over an Exponentially Stretching Curved Sheet with Variable Thermal Conductivity

By

Iqra Nasreen

RegistrationNo.:764-FBAS/MSMA/F21

Supervised by

Dr.Ambreen Afsar Khan

Department of Mathematics & Statistics
Faculty of Sciences
International Islamic University, Islamabad
Pakistan
2024

Micropolar Fluid Flow over an Exponentially Stretching Curved Sheet with Variable Thermal Conductivity

By
Iqra Nasreen

RegistrationNo.:764-FBAS/MSMA/F21

A Thesis

SubmittedinthePartialFulfillmentoftheRequirementfor the Degreeof
MASTEROFSCIENCE
In
MATHEMATICS

Supervised by

Dr.Ambreen Afsar Khan

Department of Mathematics & Statistics
Faculty of Sciences
International Islamic University, Islamabad
Pakistan
2024

Certificate

Micropolar Fluid Flow over an Exponentially Stretching Curved Sheet with Variable Thermal Conductivity

By

Iqra Nasreen

A DISSERTATION SUBMITTED IN THE PARTIAL FULFILLMENT

OF THE

REQUIREMENTS FOR THE DEGREE OF MASTER OF SCIENCE

IN MATHEMATICS

We accept this thesis as conforming to the required standard

1._____	2. _____
Prof. Dr. Nabeela Kausar	Dr. Rabia Malik
External Examiner	Internal Examiner
3._____	4. _____
Dr.Ambreen Afsar Khan	Prof. Dr.Nasir Ali
(Supervisor)	(Chairperson)

Department of Mathematics & Statistics
Faculty of Sciences
International Islamic University, Islamabad
Pakistan

2024

Thesis Certificate

The thesis entitled ***"Micropolar Fluid Flow Over an Exponentially Stretching Curved Sheet with Variable Thermal Conductivity"*** submitted by ***Iqra Nasreen, 764-FBAS/MSMA/F21*** in partial fulfillment of MS Degree in Mathematics has been completed under my guidance and supervision. I am satisfied with the quality of her research work and allow her to submit this thesis for further process to graduate with Master of Science degree from the Department of Mathematics & Statistics, as per IIUI rules and regulations.

Date……..

_____

Dr.Ambreen Afsar Khan
Associate Professor
Department of Maths & Stats
International Islamic University,
Islamabad.

Declaration

I hereby declare that this thesis, neither as a whole nor a part of it, has been copiedout from any source. It is further declared that I have prepared this dissertationentirely based on my efforts under the supervision of mysupervisor **Dr. Ambreen Afsar Khan**. No portion of the work, presented in this dissertation has been submitted in the support of any application for any degree or qualificationofthisor anyotherlearninginstitute.

Iqra Nasreen
MS(Mathematics)
Reg. No. 764-FBAS/MSMA/F21
DepartmentofMathematicsand Statistics
FacultyofSciences,
InternationalIslamicUniversityIslamabad,Pakistan.

Dedication

This thesis is dedicated to my parents

and my grandparents.

Acknowledgement

All praise and glory to **Allah Almighty** Who gave me the strength and courage to understand, learn, and complete this thesis.

I would like to express my sincere gratitude to my supervisor, my mentor, **Dr. Ambreen Afsar Khan**, for her continuous supportand guidance. Her patience, motivation, enthusiasm, and immense knowledge have been instrumental in shaping this research.

I would also like to thank my dear parents, **Mr.Zulafiqar Ali and Mrs. Nasreen Akhtar**, and my grandparents, who have always supported me. Without their unwavering support, I would not have reached the pinnacle of success. They kept me motivated and understanding, and their encouragement and guidance since my childhood have enabled me to unfold my hidden abilities.

Sincere thanks to all my friends and senior PhD research fellows for their kindness, guidance and moral support during my studies.

Lastly, I offer my regards and blessings to all of those who supported me in anyaspectduringthe completionof thisthesis.

(Iqra Nasreen)

Preface

In the past few years, many researchers have elongated their work over exponentially extended curved surfaces due to their vast applications in polymer extrusion, diagnosis of diseases, manufacturing of heat exchangers and pumps, and so on. Muhammad and Alghamdi [1] have investigated flow of Darcy Forchheimer Newtonian fluid over an exponentially extended curved surface. Kempannagari[2] examined the stagnation point motion of non-Newtonian fluid over curved surface, which is also extended exponentially. Shi et al.[3] numerically described the micropolar fluid moving over exponentially extended curved surface using the Keller box method. Kumar [4] investigated the free convective stagnation motion of non-Newtonian fluid over a curved surface, which is extended an exponentially. Alqahtani [5] extended their work to check its stability.

The Catteno-Christov equation tells us about those cases in which temperature changes rapidly and allow us to study heat transfer at microscopic level. It has numerous applications in microelectronics, laser beams, the formation of batteries, and biomedical field. Hafeez et al. [6] proposed research on Oldroyd-B fluid moving in a rotating disk. Khan [7] analyzed the flow of Carreu fluid in a slandering sheet. Rehman and Muhammad [8] examined the viscoelastic fluid over an extended surface along with soret and dufour effects. Few more efforts shedding light on Catteno-Christov can be seen through the studies [9–13].

Variable thermal conductivity helps us to deal with how corresponding material behave when temperature varies to make various heat transfer models. It is useful in fields of power generation, computer chips, and aeronautical engineering. Usman et al. [14] analyzed *Cu*-Al_2O_3/Water, which is a hybrid nanofluid moving from a permeable surface, along with the effects of radiation. Gbadeyan [15] has worked on Casson fluid flowing over a vertically flat plate along with the effects of thermal conductivity, which is variable, and viscosity. Muatafa [16] has extended the research on the flow of Maxwell fluid moving in a rotating frame. Mahmoud [17] have also worked on micropolar fluid with variable thermal conductivity.This thesis organized as follows:

Chapter one contains basic definitions.

Chapter two is a review of Ref [18]. In this chapter, the micropolar fluid flow over a curved sheet is considered.The modified Fourier's law is considered in view of the response of heat transfer.

Chapter three discusses the microploar fluid over an exponentially stretching sheet. Variable thermal conductivity is taken as temperature-dependent. For all the relevant parameters, the physical understandings of the flow quantities are studied.

Contents

1 Preliminaries **3**

1.1 Fluid . . . 3

1.2 Fluid Mechanics . . . 3

1.3 Fluid Properties . . . 3

1.3.1 Pressure . . . 3

1.3.2 Viscosity . . . 4

1.3.3 Density . . . 4

1.4 Types of Fluids . . . 4

1.4.1 Inviscid Fluid . . . 4

1.4.2 Real Fluid . . . 4

1.4.3 Newtonian Fluid . . . 4

1.4.4 Non-Newtonian Fluid . . . 5

1.5 Types of Flows . . . 5

1.5.1 Steady Flow . . . 5

1.5.2 Unsteady Flow . . . 5

1.5.3 Compressible Flow . . . 5

1.5.4 Incompressible Flow . . . 5

1.5.5 Rotational Flow . . . 5

1.5.6 Irrotational Flow . . . 6

1.6 Fundamental Laws . . . 6

1.6.1 Continuity Equation . . . 6

1.6.2 Law of Conservation of Momentum . . . 6

1.6.3 Catteno-Christov Heat Flux Model 6
1.7 Non-dimensional Parameters 7
1.7.1 Prandtl Number 7
1.7.2 Magnetic Parameter 7
1.8 Micropolar Fluid 7
1.9 Solution Methodology 8

2 Study of Non-Newtonian Fluid over a Curve Stretching Surface 9
2.1 Mathematical Formulation 9
2.2 Solution of the Problem 12
2.2.1 Zeroth Order Deformation 12
2.2.2 Ith Order Deformation 14
2.2.3 Convergence of Solution 15
2.2.4 Results and Discussion 16
2.3 Conclusions 17

3 Micropolar Fluid Flow over an Exponentially Stretching Curved Sheet with Variable Thermal Conductivity 23
3.1 Mathematical Formulation 24
3.1.1 Results and Discussion 28
3.2 Conclusion 38

Chapter 1

Preliminaries

Some fundamental definitions of fluid mechanics have been covered in order to better grasp the further concepts in this chapter.

1.1 Fluid

Any substance that flows when shear stress is applied, it does not have any specific shape and it shape changes when external force is applied. Liquid and gases such as water, gasoline, and ketchup are examples of fluid.

1.2 Fluid Mechanics

It is field of physics concerned with the investigation of fluid either at rest or in motion.

1.3 Fluid Properties

1.3.1 Pressure

Pressure is defined as the proportion of force to an area. Mathematically, it is represented as

$$P = \frac{\left|\vec{F}\right|}{A}, \tag{1.1}$$

where $\left|\vec{F}\right|$ the magnitude of force and area is denoted by A.

1.3.2 Viscosity

It determines the amount of resistance or friction in fluid flow. Mathematically, it is expressed as

$$\mu = \frac{\text{Shear Stress}}{\text{Shear Strain}} = \frac{\tau}{(\frac{du}{dy})}. \tag{1.2}$$

1.3.3 Density

Density defines mass in terms of unit volume. Mathematically it is shown as

$$\rho = \frac{m}{V}, \tag{1.3}$$

where V and m stand for volume and mass, respectively.

1.4 Types of Fluids

1.4.1 Inviscid Fluid

It is defined as fluid with zero viscosity ($\mu = 0$). They donot exist in nature.

1.4.2 Real Fluid

The fluid which have non zero viscosity is said to be a real fluid.

1.4.3 Newtonian Fluid

The viscosity of fluid remains unaffected by shear rate i.e., it obeys law of viscosity given by Newton. Mathematically it is represented as

$$\tau = \upsilon \frac{du}{dy}, \tag{1.4}$$

where $\frac{du}{dy}$ shows shear rate and υ shows the viscosity. Water and alcohol are examples of Newtonian fluid.

1.4.4 Non-Newtonian Fluid

If a fluid deviates from Newton's viscosity law, it is known as Non-Newtonian fluid. Mathematically,

$$\tau = \kappa \left(\frac{du}{dy}\right)^n, n \neq 0, 1, \tag{1.5}$$

where κ is stability parameter and n is power law parameter. Some examples of Non-Newtonian fluids are butter, cheese, and paint etc.

1.5 Types of Flows

1.5.1 Steady Flow

A flow of fluid in which velocity and other characteristics donot vary w.r.t. time is known as steady flow. Mathematically,

$$\frac{\partial p}{\partial t} = \frac{\partial v}{\partial t} = ... = 0. \tag{1.6}$$

1.5.2 Unsteady Flow

In unsteady flow the characteristics of fluid like pressure, density, and velocity at specific point vary w.r.t. time.

1.5.3 Compressible Flow

If density of fluid donot remains the same, it varies during the flow is known as compressible fluids.

1.5.4 Incompressible Flow

In the incompressible flow density of fluid doesnot vary throughout the flow.

1.5.5 Rotational Flow

When fluid particles spin about their own center of mass is called rotational flow.

1.5.6 Irrotational Flow

When fluid is moving then no particle of fluid rotate in any direction then it is known as irrotational flow.

1.6 Fundamental Laws

1.6.1 Continuity Equation

It is called as law of conservation of mass. According to this law, the amount of mass entering the body is equal to amount of mass leaving the body. Mathematically,

$$\nabla.(\rho\mathbf{V}) + \frac{\partial p}{\partial t} = 0, \tag{1.7}$$

where $\mathbf{V}$ denotes velocity, ρ denotes density and t is time. When density is constant then Eq. (1.7) takes the following form

$$\nabla.\mathbf{V} = 0. \tag{1.8}$$

1.6.2 Law of Conservation of Momentum

This law asserts that the total of all external forces equals to the rate at which a body's linear momentum changes over time. Mathematically,

$$\rho\frac{d\mathbf{V}}{dt} = \operatorname{div}\tau + \rho\mathbf{b}, \tag{1.9}$$

where material time derivative is represented by $\frac{d}{dt}$, τ and b are body forces and Cauchy stress tensor respectively.

1.6.3 Catteno-Christov Heat Flux Model

This model is modification of Fourier's law in which the thermal relaxation time characteristic has been taken into account. Its equation is represented as

$$q^{\circ} + \lambda^{*}(\frac{\partial q}{\partial t} + \mathbf{V}.\nabla q^{\circ} - q^{\circ}.\nabla\mathbf{V} + (\nabla.\mathbf{V})q^{\circ}) = -\widetilde{k}\nabla T \tag{1.11}$$

here c_p describes the specific heat of fluid at constant pressure,$\widetilde{k}$ shows thermal conductivity, λ^* represents thermal relaxation time and density is denoted by ρ.

1.7 Non-dimensional Parameters

1.7.1 Prandtl Number

It is obtained by dividing the momentum diffusivity by thermal diffusivity. It can be expressed as:

$$\mathrm{Pr} = \frac{\mu c_p}{k}, \tag{1.12}$$

where μ represents dynamic viscosity, c_p shows specific heat and k describes thermal conductivity.

1.7.2 Magnetic Parameter

The ratio of electromagnetic forces to inertial forces is defined as magnetic parameter

$$M = \frac{\sigma B^2 L_C}{U\rho}, \tag{1.13}$$

where L_C, σ, B, ρ, and U are characteristic length, electric conductivity, magnetic field, density and velocity respectively.

1.8 Micropolar Fluid

It belong to class of Newtonian fluid which exhibit some special microscopic properties that is due to the rotation of its fluid particles along their center of mass and due this rotational flow of particles micropolar fluid posses both couple stress and body stress. Their behavior is also effected by microstructure present in them. The stress tensor τ_{ij} and couple stress tenor c_{ij} is represented as

$$\tau_{ij} = (2\mu + k)\, d_{ij} + (\operatorname{div} \mathbf{V} - p)\, \omega_{ij} + k\varepsilon_{ijk}\, (\lambda - N)\,, \tag{1.14}$$

$$c_{ij} = \beta\lambda_{i,j} + (\alpha \operatorname{div} \mathbf{V})\, \omega_{ij} + \gamma\lambda_{j,i}, \tag{1.15}$$

where d_{ij} represents strain rate component, N shows the microrotation vector, λ represents vorticity vector, ω_{ij} is known as Kronecker delta, k is coefficient of vortex viscosity and gyro-viscosity coefficients are represented by α, β, γ.

1.9 Solution Methodology

We have used ND-Solve technique to solve our nonlinear complex coupled ODEs, it is a built in command in mathematica.

Chapter 2

Study of Non-Newtonian Fluid over a Curve Stretching Surface

In this chapter, we basically focused on micropolar fluid is flowing over a curved sheet that is stretched, along with the effects of Cattaneo-Christov heat flux model and MHD. By modelling the governing equations of fluid in curvilinear coordinates, we obtained non-linear, complicated PDEs. After using specific transformations, we get non-linear coupled ODEs. After that, we apply OHAM to solve these complex, non-linear, and coupled ODES. Then we examined the parameters that are involved and also studied them graphically.

2.1 Mathematical Formulation

Consider a steady and incompressible micropolar fluid across a stretched curved sheet. The fluid is flowing in a circle whose radius is R°. Assuming the fluid which is electrically conducting with constant magnetic field represented by B_0, which is directed in r-axis. T_W is the surface temperature, where $T_W \succcurlyeq T_\infty$ is temperature of surroundings. Using these assumptions, the governing equation for micropolar fluid and energy equation are as follows:

$$R^{\circ}\frac{\partial u}{\partial x} + (R^{\circ} + r)\frac{\partial v}{\partial r} + v = 0, \tag{2.1}$$

$$\frac{u^2}{R^{\circ} + r} = \frac{1}{\rho}\frac{\partial P}{\partial r}, \tag{2.2}$$

$$\frac{R^{\circ}u}{R^{\circ}+r}\frac{\partial u}{\partial x}+v\frac{\partial u}{\partial r}+\frac{uv}{R^{\circ}+r} = -\frac{1}{\rho}\frac{R^{\circ}}{R^{\circ}+r}\frac{\partial P}{\partial x}+\left(\nu^{*}+\frac{K}{\rho}\right)\left(\frac{\partial^{2}u}{\partial r^{2}}+\frac{1}{R^{\circ}+r}\frac{\partial u}{\partial r}-\frac{u}{(R^{\circ}+r)^{2}}\right) \frac{K}{\rho}\frac{\partial N}{\partial r}-\sigma\frac{B_{0}^{2}}{\rho}u, \tag{2.3}$$

$$\frac{R^{\circ}u}{R^{\circ}+r}\frac{\partial N}{\partial x}+v\frac{\partial N}{\partial r}=\frac{\zeta}{\rho j}\left(\frac{\partial^{2}N}{\partial r^{2}}+\frac{1}{R^{\circ}+r}\frac{\partial N}{\partial r}\right)-\frac{K}{\rho j}\left(\frac{\partial u}{\partial r}+\frac{u}{R^{\circ}+r}+2N\right), \tag{2.4}$$

$$v\frac{\partial T}{\partial r}+\frac{R^{\circ}u}{R^{\circ}+r}\frac{\partial T}{\partial x}+\alpha\left(\begin{array}{c} v^{2}\frac{\partial^{2}T}{\partial r^{2}}+\frac{R^{\circ}u}{R^{\circ}+r}\frac{\partial u}{\partial r}\frac{\partial T}{\partial x}+\frac{R^{\circ 2}u^{2}}{(R^{\circ}+r)^{2}}\frac{\partial^{2}T}{\partial x^{2}} \\ -v\frac{\partial v}{\partial r}\frac{\partial T}{\partial r}-\frac{R^{\circ}uv}{R^{\circ}+r}\frac{\partial T}{\partial x}+\frac{2R^{\circ}uv}{R^{\circ}+r}\frac{\partial^{2}T}{\partial x\partial r} \end{array}\right)=\frac{\kappa}{\rho c_{p}}\left(\frac{1}{R^{\circ}+r}\frac{\partial T}{\partial r}+\frac{\partial^{2}T}{\partial r^{2}}\right), \tag{2.5}$$

where j is micro-inertia, u is the velocity component in x direction and v is in r direction, P represents the pressure, σ shows the electric conductivity, ς represents the spin gradient viscosity, T represents the temperature, vortex viscosity is denoted by K, N shows the microrotation parameter, ν^{*} is kinematic viscosity, ρ describes the fluid density, thermal conductivity is denoted by κ and α shows the thermal relaxation time.

The boundary conditions are given as:

$$\begin{aligned} u &= ax,\ N=-m_{0}\frac{\partial u}{\partial r},\ v=0,\quad T=T_{w}\ \text{ at } r=0,\\ u &\to 0,\quad \frac{\partial u}{\partial r}\to 0,\quad N\to 0,\quad T\to T_{\infty}\quad \text{at}\ \ r\to\infty, \end{aligned} \tag{2.6}$$

where $m_{0}(0\leq m_{0}\leq 1)$ is constant.

Using the following dimensionless transformation

$$\begin{aligned} u &= axf'(\eta), v=-\frac{R'}{R'+r}\sqrt{\nu^{*}a}f(\eta), N=ax\sqrt{\frac{a}{\nu^{*}}}g,\\ \eta &= \sqrt{\frac{a}{\nu^{*}}}r, P=\rho a^{2}x^{2}P(\eta), \theta(\eta)=\frac{T-T_{\infty}}{T_{w}-T_{\infty}}, \end{aligned} \tag{2.7}$$

after using these transformations, Eq. (2.1) is identically satisfied and Eqs. (2.2) to (2.5) become

$$\frac{\partial P}{\partial \eta}=\frac{f'^{2}}{\omega+\eta}, \tag{2.8}$$

$$\frac{2\omega}{\omega+\eta} = (1+W)\left[f''' + \frac{f''}{\omega+\eta} - \frac{f'}{(\omega+\eta)^2}\right] + \frac{\omega}{\omega+\eta} f f'' - S g' - M^2 f' + \frac{\omega}{\omega+\eta} f'^2 + \frac{\omega}{(\omega+\eta)^2} f f', \tag{2.9}$$

$$\left(\frac{W}{2}+1\right)\left[g'' + \frac{1}{\omega+\eta} g'\right] = W\left(\frac{f'}{\omega+\eta} + 2g + f''\right) - \frac{\omega}{\omega+\eta} f g' + \frac{\omega}{\omega+\eta} g f', \tag{2.10}$$

$$\left(\theta'' + \frac{\theta'}{\omega+\eta}\right) + \Pr \frac{\omega}{\omega+\eta} f\ \theta' = \frac{\gamma\omega}{\omega+\eta} \Pr\left[f^2\theta' - f f'\theta' + f^2\theta''\right], \tag{2.11}$$

$$W = \frac{K}{\nu^*}, \quad \omega = R'\sqrt{\frac{a}{\nu^*}}, \quad \gamma = a\alpha, \quad M = \sqrt{\frac{\sigma}{\rho a}} B_{0,} \quad \Pr = \frac{\mu c_p}{\kappa}, \tag{2.12}$$

where W and ω are the material and curvature parameters respectively, thermal relaxation time is denoted by γ, Pr represents the Prandtl number and M^2 is magnetic parameter.

The non dimensional form of boundary conditions will be

$$\begin{aligned} f(0) &= 0 = g(0),\ \theta(0) = 1,\ f'(0) = 1, \\ f'(\infty) &= 0,\ g(\infty) = 0,\ \theta(\infty) = 0. \end{aligned} \tag{2.13}$$

Now removing pressure term between Eqs. (2.8) and (2.9), we get

$$f^{iv} + \frac{f'}{(\omega+\eta)^3} + \frac{2}{\omega+\eta} f''' - \frac{\omega}{\omega+\eta}(f''f' - f f''') - \frac{1}{(\omega+\eta)^2} f'' - \frac{\omega}{(\omega+\eta)^3} f' f - \frac{\omega}{(\omega+\eta)^2}(f'^2 - f f'') - M^2\left(f'' + \frac{f'}{\omega+\eta}\right) = 0. \tag{2.14}$$

The expression of pressure is

$$P = \left[(1+W)\left\{f''' + \frac{1}{\omega+\eta} f'\left(1 - \frac{1}{\omega+\eta}\right)\right\} - \frac{\omega}{\omega+\eta} f'^2 + \frac{\omega}{\omega+\eta} f'' f + \frac{\omega}{(\omega+\eta)^2} f f' - W g' - M^2 f'\right]. \tag{2.15}$$

The coefficients of skin friction and Couple stress are defined as

$$C_f = \frac{T_{rs}}{\rho u_w^2},\ C_m = \frac{M_w}{\mu j u_w}, \tag{2.16}$$

where M_w is the wall Couple stress and T_{rs} is the wall stress given as

$$\begin{aligned} T_{rs} &= (\mu + K)(\frac{\partial u}{\partial r} - \frac{u}{r + R'}) + KN \mid_{r=0}, \\ M_w &= \zeta \frac{\partial N}{\partial r} \mid_{r=0}, \end{aligned} \tag{2.17}$$

2.2 Solution of the Problem

We have solved our equations by using OHAM. Initially, we defined a set of base function $\{\eta^k e^{-n\eta}/k \geq 0, n \geq 0\}$, as follow:

$$f(\eta) = a^0_{0,0} + \sum_{n=0}^{\infty} \sum_{k=0}^{\infty} a^k_{l,n} \eta^k e^{-\eta n}, \tag{2.19}$$

$$g(\eta) = \sum_{n=0}^{\infty} \sum_{k=0}^{\infty} b^k_{l,n} \eta^k e^{-\eta n}, \tag{2.20}$$

$$\theta(\eta) = \sum_{n=0}^{\infty} \sum_{k=0}^{\infty} c^k_{l,n} \eta^k e^{-\eta n}, \tag{2.21}$$

where $a^k_{l,n}$, $b^k_{l,n}$, $c^k_{l,n}$ are coefficients. We choose initial guess and linear operators as follow

$$\begin{aligned} L_f &= \frac{d^4}{d\eta^4} - \frac{d^3}{d\eta^3}, \\ Lg &= \frac{d^2}{d\eta^2} - 1, \quad L_\theta = \frac{d^2}{d\eta^2} - 1, \end{aligned} \tag{2.22}$$

$$f_0(\eta) = 1 - e^{-\eta}, g_0(\eta) = \eta e^{-\eta}, \theta_0(0) = e^{-\eta}, \tag{2.23}$$

$$\begin{aligned} L_f &= \left[C_1 + C_2 y + C_3 y^2 + C_{4e^{-\eta}}\right], \\ L_g &= \left[C_5 + C_{6e^{-\eta}}\right], \quad L_\theta = \left[C_7 + C_{8e^{-\eta}}\right]. \end{aligned} \tag{2.24}$$

2.2.1 Zeroth Order Deformation

$$(1-t) L_f \left[\widetilde{f}(\eta, t) - f_0(\eta)\right] = t c^f_0 N_f \left[\widetilde{f}(\eta, t)\right], \tag{2.25}$$

$$(1-t) L_g \left[\widetilde{g}(\eta, t) - g_0(\eta)\right] = t c^g_0 N_g \left[\widetilde{g}(\eta, t), \widetilde{f}(\eta, t)\right], \tag{2.26}$$

$$(1-t)L_\theta\left[\widetilde{\theta}(\eta,t)-\theta_0(\eta)\right]=tc_0^\theta N_\theta\left[\widetilde{\theta}(\eta,t),\widetilde{f}(\eta,t)\right], \tag{2.27}$$

$$\begin{aligned}\widetilde{f}(\eta,t) &= 0,\ \frac{\partial\widetilde{f}(\eta,t)}{\partial\eta}=1,\ \widetilde{\theta}(\eta,t)=1,\ \ \widetilde{g}(\eta,t)=0,\ \ \text{at}\ \ \eta=0\\ \frac{\partial\widetilde{f}(\eta,t)}{\partial\eta} &= 0,\ \frac{\partial^2\widetilde{f}(\eta,t)}{\partial\eta^2}=0,\widetilde{g}(\eta,t)=0,\widetilde{\theta}(\eta,t)=0,\ \ \text{at}\ \ \ \eta=\infty,\end{aligned} \tag{2.28}$$

where auxiliary parameters c_0^f, c_0^g, c_0^θ and nonlinear operators N_f, N_g, N_θ are defined as

$$\begin{aligned}N_f\left[\widetilde{f}(\eta,t)\right] &= \widetilde{f}^{iv}(\eta,t)+\frac{\widetilde{f}^{'''}(\eta,t)}{(\omega+\eta)}-\frac{\widetilde{f}^{''}(\eta,t)}{(\omega+\eta)^2}-\frac{\omega}{(\omega+\eta)}\left(\widetilde{f}^{'}(\eta,t)\widetilde{f}^{''}(\eta,t)-\widetilde{f}^{'''}(\eta,t)\widetilde{f}(\eta,t)\right)\\ &+\frac{\widetilde{f}^{'}(\eta,t)}{(\omega+\eta)^3}-\frac{\omega}{(\omega+\eta)^2}\left(\widetilde{f}^{'2}(\eta,t)-\widetilde{f}^{'}(\eta,t)\widetilde{f}^{''}(\eta,t)\right)\\ &-\frac{\omega}{(\omega+\eta)^3}\widetilde{f}^{'}(\eta,t)\widetilde{f}(\eta,t)-M^2\frac{\widetilde{f}^{'}(\eta,t)}{(\omega+\eta)}-M^2\widetilde{f}^{''}(\eta,t),\end{aligned} \tag{2.29}$$

$$\begin{aligned}N_f\left[\widetilde{g}(\eta,t),\widetilde{f}(\eta,t)\right] &= \left(1+\frac{W}{2}\right)\left[\frac{\widetilde{g}^{'}(\eta,t)}{(\omega+\eta)}+\widetilde{g}^{''}(\eta,t)\right]-\frac{\omega}{(\omega+\eta)}\left(\widetilde{f}^{'}(\eta,t)\widetilde{g}(\eta,t)-\widetilde{g}^{'}(\eta,t)\widetilde{f}(\eta,t)\right)\\ &-W\left(\frac{\widetilde{f}^{'}(\eta,t)}{(\omega+\eta)}+2\widetilde{g}(\eta,t)+\widetilde{f}^{''}(\eta,t)\right),\end{aligned} \tag{2.30}$$

$$\begin{aligned}N_f\left[\widetilde{\theta}(\eta,t),\widetilde{f}(\eta,t)\right] &= -\frac{\omega\zeta}{(\omega+\eta)^2}\Pr\left(\begin{array}{c}\widetilde{\theta}^{''}(\eta,t)\widetilde{f}(\eta,t)\widetilde{f}(\eta,t)-\widetilde{\theta}^{'}(\eta,t)\widetilde{f}(\eta,t)\widetilde{f}^{'}(\eta,t)\\ +\widetilde{\theta}^{'}(\eta,t)\widetilde{f}(\eta,t)\widetilde{f}(\eta,t)\end{array}\right)\\ &+\widetilde{\theta}^{''}(\eta,t)+\Pr\frac{\omega}{(\omega+\eta)}\widetilde{\theta}^{'}(\eta,t)\widetilde{f}(\eta,t)+\frac{\widetilde{\theta}(\eta,t)}{(\omega+\eta)},\end{aligned} \tag{2.31}$$

when $t=0$ and $t=1$

$$\begin{aligned}\widetilde{f}(\eta,0) &= f_0(\eta),\ \widetilde{\theta}(\eta,0)=\theta_0(\eta),\ \widetilde{g}(\eta,0)=g_0(\eta),\\ f(\eta) &= \widetilde{f}(\eta,1),\ \ \widetilde{g}(\eta,1)=g(\eta),\ \widetilde{\theta}(\eta,1)=\theta(\eta).\end{aligned} \tag{2.32}$$

Expand $\widetilde{\theta}(\eta,t)$, $\widetilde{f}(\eta,t)$ and $\widetilde{g}(\eta,t)$ in Taylor's series as

$$\widetilde{f}(\eta,t)=f_0(\eta)+\sum_{l=1}^{\infty}f_l(\eta)\,t^l, \tag{2.33}$$

$$\widetilde{g}(\eta,t)=g_0(\eta)+\sum_{l=1}^{\infty}g_l(\eta)\,t^l, \tag{2.34}$$

$$\widetilde{\theta}(\eta,t)=\theta_0(\eta)+\sum_{l=1}^{\infty}\theta_l(\eta)\,t^l, \tag{2.35}$$

where

$$f_l(\eta)=\frac{1}{l!}\frac{\partial\widetilde{f^l}(\eta,t)}{\partial t^l}\mid_{t=0},\ g_l(\eta)=\frac{1}{l!}\frac{\partial\widetilde{g^l}(\eta,t)}{\partial t^l}\mid_{t=0},\ \theta_l(\eta)=\frac{1}{l!}\frac{\partial\widetilde{\theta^l}(\eta,t)}{\partial t^l}\mid_{t=0,} \tag{2.36}$$

when $t=1$ series converges and thus

$$f(\eta)=f_0(\eta)+\sum_{l=1}^{l}f_k(\eta),\ g(\eta)=g_0(\eta)+\sum_{l=1}^{l}g_k(\eta),\ \theta(\eta)=\theta_0(\eta)+\sum_{l=1}^{l}\theta_k(\eta). \tag{2.37}$$

2.2.2 Ith Order Deformation

$$\begin{aligned}
&L_f\left[f_1(\eta)-\chi_l f_{l-1}(\eta)=c_0^f R_{1l}(\eta)\right],\\
&L_g\left[g_1(\eta)-\chi_l g_{l-1}(\eta)=c_0^g R_{1l}(\eta)\right],\\
&L_\theta\left[\theta_1(\eta)-\chi_l\theta_{l-1}(\eta)=c_0^\theta R_{1l}(\eta)\right],
\end{aligned} \tag{2.38}$$

$$\begin{aligned}
f_l(0) &= 0,\ \frac{\partial f_l(0)}{\partial\eta}=1,\ \theta_l(0)=1,\ g_l(0)=0,\\
\frac{\partial f_l(\infty)}{\partial\eta} &= 0,\ \frac{\partial^2 f_l(\infty)}{\partial\eta^2}=0,\ \theta_l(\infty)=0,\ g_l(\infty)=0,
\end{aligned} \tag{2.39}$$

where

$$
\begin{aligned}
R_{1l}(\eta) &= \tilde{f}_l^{iv} + \frac{2f_l^{iv}}{(\omega+\eta)} - \frac{f_l'''}{(\omega+\eta)^2} - \frac{\omega}{(\omega+\eta)}\left(\sum_{k=0}^{l} f_k' f_{l-k}'' - \sum_{k=0}^{l} f_k f_{l-k}'''\right) \\
&\quad -\frac{\omega}{(\omega+\eta)^2}\left(\sum_{k=0}^{l} f_k' f_{l-k}' - \sum_{k=0}^{l} f_k f_{l-k}''\right) - \frac{\omega}{(\omega+\eta)^3}\sum_{k=0}^{l} f_k f_{l-k}' \\
&\quad -M^2\left(f_l'' + \frac{f_l'}{(\omega+\eta)}\right), \qquad (2.40)
\end{aligned}
$$

$$
R_{2l}(\eta) = \left(\frac{W}{2}+1\right)\left[g_l'' + \frac{g_l'}{(\omega+\eta)}\right] + \frac{\omega}{(\omega+\eta)}\sum_{k=0}^{l} f_l g_{l-k} - S\left(2g_l + f_l'' + \frac{f_l'}{(\omega+\eta)}\right), \qquad (2.41)
$$

$$
\begin{aligned}
R_{3l}(\eta) &= \theta_l'' + \frac{\theta_l'}{(\omega+\eta)} + \Pr\frac{\omega}{(\omega+\eta)}\sum_{k=0}^{l}\theta_l' f_{l-k} \\
&\quad -\frac{\omega\gamma}{(\omega+\eta)}\Pr\sum_{k=0}^{l}\left[f_{l-k}\left(\sum_{k=0}^{l}\theta_m' f_{k-l} - \theta_m' f_{k-l}' + \theta_m'' f_{k-l}\right)\right]. \qquad (2.42)
\end{aligned}
$$

2.2.3 Convergence of Solution

In series solution, the auxiliary parameters are c_0^f, c_0^g and c_0^θ, they are used to find rate of homotopy series solution and region of convergence, values of c_0^f, c_0^g and c_0^θ are found by using average residual error which is defined as

$$
E_f = \int_0^\infty \left\{ \begin{array}{c} f^{iv} + \frac{1}{(\omega+\eta)^3}f' + \frac{2}{\omega+\eta}f''' - \frac{\omega}{\omega+\eta}(f''f' - ff''') - \frac{f''}{(\omega+\eta)^2} - \frac{\omega}{(\omega+\eta)^3}ff' - \\ \frac{\omega}{(\omega+\eta)^2}(f'^2 - ff'') - M^2(f'' + \frac{f'}{\omega+\eta}) \end{array} \right\}^2 d\eta, \qquad (2.43)
$$

$$
E_g = \int_0^\infty \left\{ \left(1+\frac{S}{2}\right)\left[g'' + \frac{1}{\omega+\eta}g'\right] + \frac{\omega}{\omega+\eta}(g'f - gf') - W\left(2g + f'' + \frac{f'}{\omega+\eta}\right) \right\}^2 d\eta, \qquad (2.44)
$$

$$
E_\theta = \int_0^\infty \left\{ \left[\frac{\theta'}{\omega+\eta} + \theta''\right] + \Pr\frac{\omega}{\omega+\eta}\theta f' - \Pr\frac{\gamma\omega}{(\omega+\eta)^2}\left(f^2\theta' + f'f\theta' + f^2\theta'\right) \right\}^2 d\eta. \qquad (2.45)
$$

$Order$	E_f	E_g	E_θ
2	1.75962×10^{-2}	0.944391	8.9332×10^{-3}
6	1.71826×10^{-8}	3.36992×10^{-5}	1.55282×10^{-4}
8	2.20361×10^{-11}	3.26767×10^{-5}	2.92079×10^{-5}
10	3.44720×10^{-14}	4.02019×10^{-6}	6.19870×10^{-6}
16	1.97829×10^{-22}	2.88390×10^{-8}	9.19519×10^{-8}
18	1.00031×10^{-24}	7.44161×10^{-9}	2.45420×10^{-8}
20	3.12892×10^{-27}	2.05989×10^{-9}	6.92849×10^{-9}
22	9.26099×10^{-30}	5.9870×10^{-10}	1.98332×10^{-9}
26	1.53241×10^{-34}	5.60159×10^{-11}	1.72688×10^{-10}
28	6.43949×10^{-35}	1.78228×10^{-11}	5.2213×10^{-11}
30	2.60758×10^{-30}	5.79461×10^{-12}	1.59839×10^{-11}

Table 2.1: Square residual error

2.2.4 Results and Discussion

We have computed graphically the impacts of the parameters that appeared in the above equations in Figs 2.1 to 2.12. Fig 2.1 shows that if we rise the value of M which represents the magnetic parameter, the velocity $f^{'}(\eta)$ decreases because magnetic field is a force which cause resistance, this results reduction in velocity profile. In Fig 2.2, we examined the influence of material parameter on velocity. They have direct relation as W increases, velocity profile $f^{'}(\eta)$ also increases. Fig 2.3 shows the influence of curvature ω on $f^{'}(\eta)$. The velocity extends with increase in curvature. Fig 2.4 demonstrates the effect of microrotation parameter $g(\eta)$ when magnetic force M is changed. It shows that $g(\eta)$ decreases as we increase the value of magnetic force. Fig 2.5 demonstrates the effect of curvature ω on the microrotation parameter $g(\eta)$, this graph depicts that as curvature rises $g(\eta)$ also increases. Fig 2.6 illustrates the impact of material parameter W on $g(\eta)$. We observed that mirorotation rises with rising values of S. Fig 2.7 describes the effect of temperature profile $\theta(\eta)$ on Prandtl number. The graph shows that by increasing Pr, the $\theta(\eta)$ declines. Fig 2.8 depicts the effect of thermal relaxation parameter

γ on $\theta(\eta)$, the $\theta(\eta)$ reduces by enhancing the thermal relaxation parameter. Fig 2.9 describes the impact of curvature on $\theta(\eta)$. We have seen that $\theta(\eta)$ increases with increasing in ω. Fig 2.10 demonstrates the effect of M on the pressure of a fluid, by rising the value of M pressure reduces. Fig 2.11 is plotted to show the influence of curvature parameter on the pressure. We have seen that by increasing ω pressure also increases. Fig 2.12 illustrates the same effect as in Fig 2.10 when material parameter W changes.

Tables 2.2, 2.3 and 2.4 are calculated to analyze the numerical results of skin friction, couple stress, and rate of heat transfer for various values of M, ω and S. From Table 2.2, it is shown that the value of skin friction reduces by increasing the value of curvature, and if we rise the value of M and S skin friction value also increases. It is observed from Table 2.3 that stress tensor coefficient increases when value of M and S rises, while keeping the value of ω constant. Table 2.4 illustrates that rate at which heat transfer increases by rising the value of Pr and γ.

2.3 Conclusions

In this chapter, we analyze the flow of micropolar fluid across a stretched curved sheet with MHD effects. The Cattaneo-Christov model has also been applied to check thermal effects. The following observations have been shown by graphical results:

(1) By rising the values of ω, M, and S, the pressure distribution value also enhances.

(2) By enhancing the value of M,the microrotation and velocity distribution reduces.

(3) The temperature is reduced by rising the γ parameter.

(4) By enhancing the curvature value, the microrotation and velocity also increases.

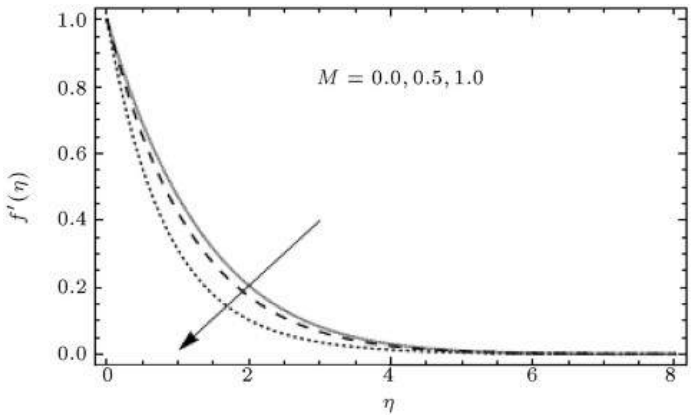

Fig 2.1: Influence of M via $f^{'}(\eta)$ when $W = 1$ and $\omega = 7$.

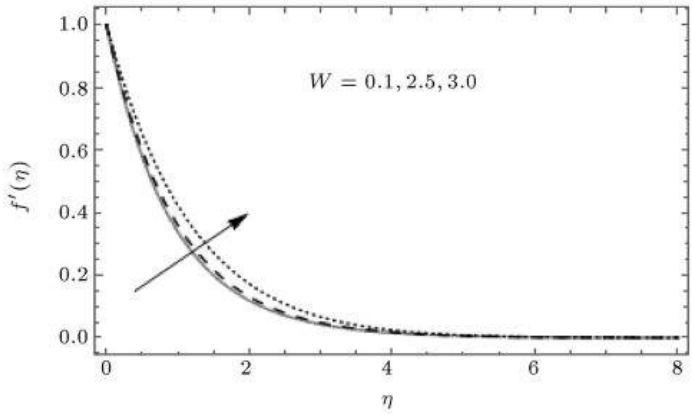

Fig 2.2: Influence of W via $f^{'}(\eta)$ when $M = 0.5$ and $\omega = 7$.

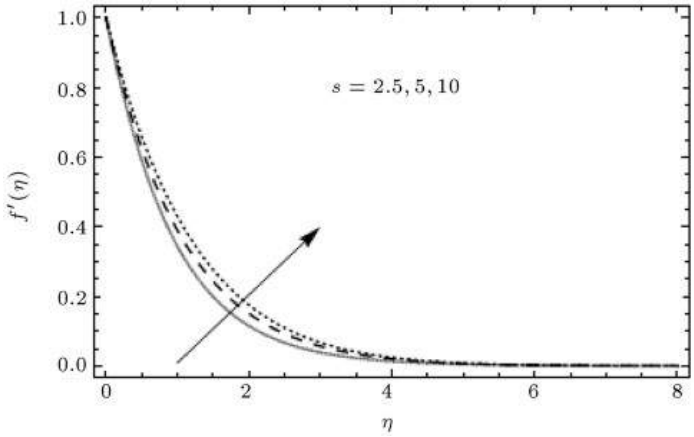

Fig 2.3: Influence of curvature via $f^{'}(\eta)$ when $M = 0.8$ and $W = 1$.

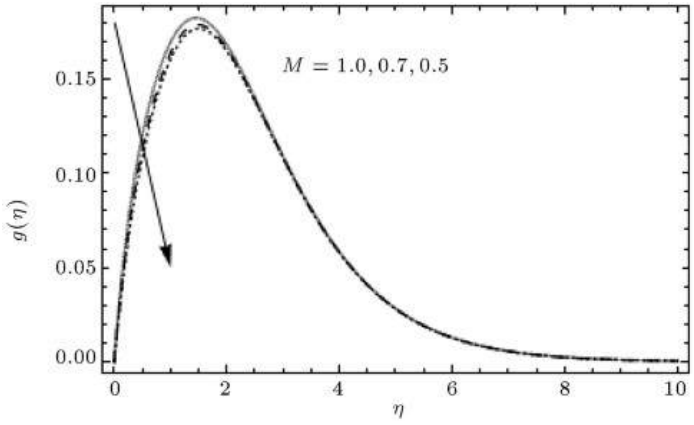

Fig 2.4: Influence of M via $g(\eta)$ when $\omega = 7$ and $W = 1$.

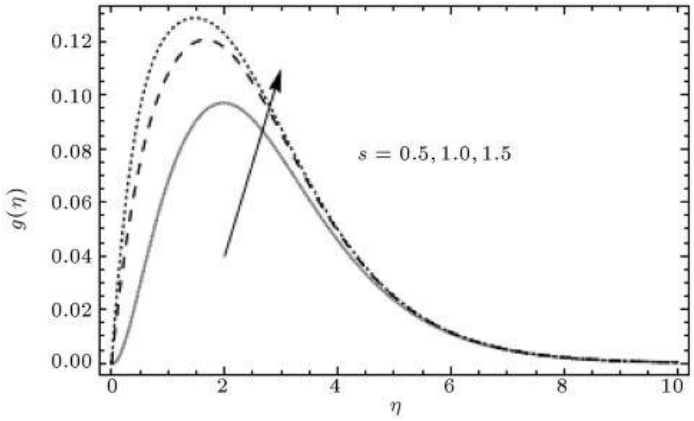

Fig 2.5: Influence of curvature via $g(\eta)$ when $W = 3$ and $M = 0.8$.

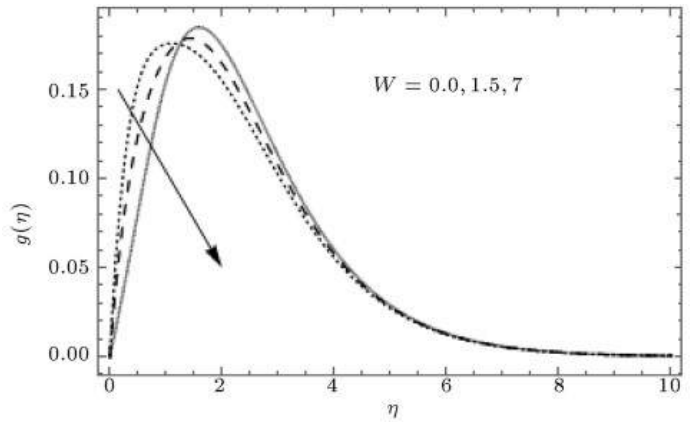

Fig 2.6: Influence of W via $g(\eta)$ when $\omega = 7$ and $M = 0.8$.

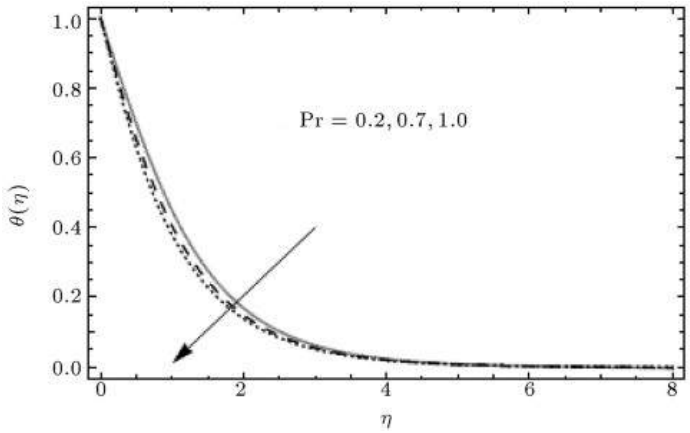

Fig 2.7: Influence of Prandtl via $\theta(\eta)$ when $\omega = 7$ and $\gamma = 0.5$.

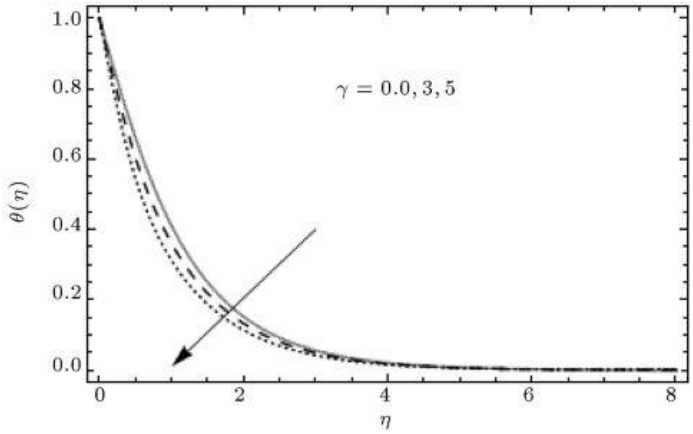

Fig 2.8: Influence of thermal relaxation via $\theta(\eta)$ when $\omega = 7$ and $\mathrm{Pr} = 1$.

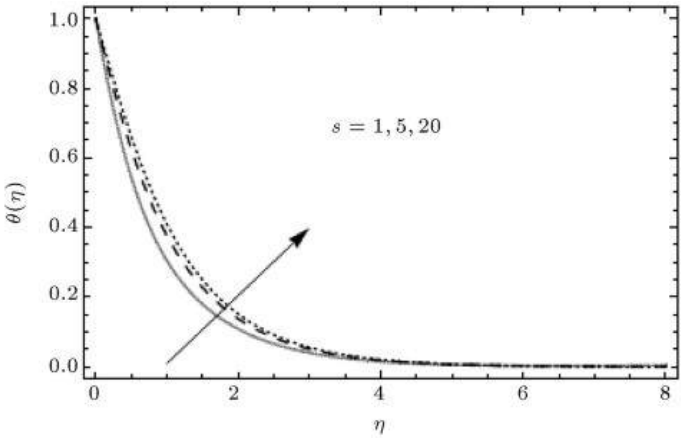

Fig 2.9: Influence of curvature via $\theta(\eta)$ when $W = 2.5$ and $\gamma = 0.6$.

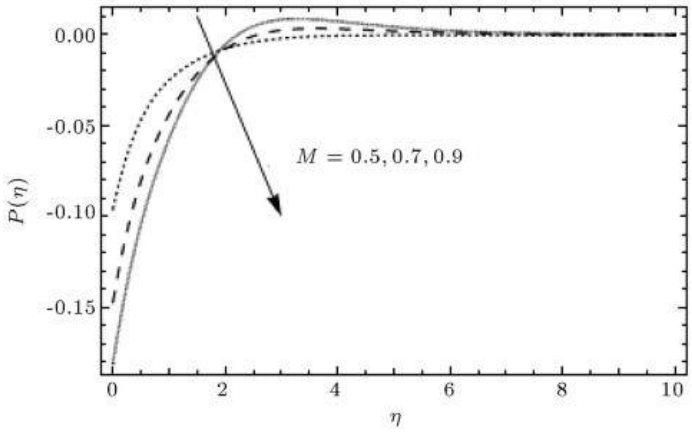

Fig 2.10: Influence of M via pressure when $W = 7$ and $\omega = 0.5$.

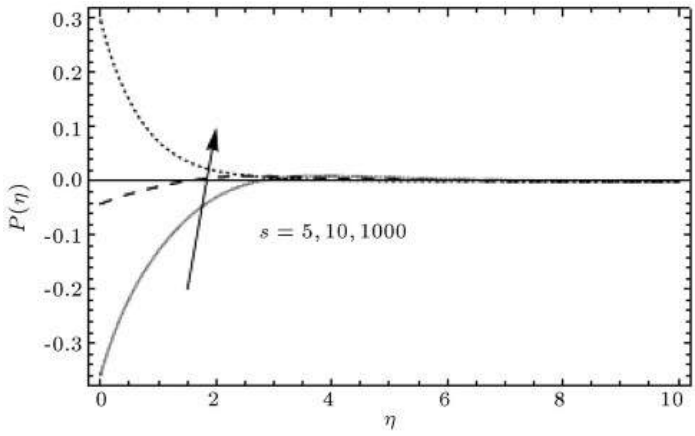

Fig 2.11: Influence of curvature via pressure when $M = 1.5$ and $W = 0.5$.

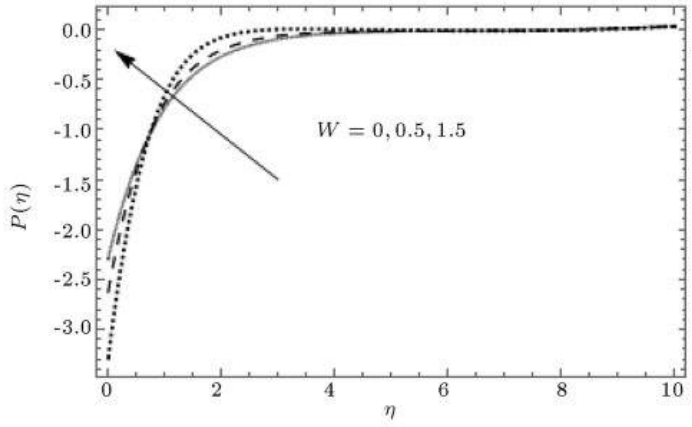

Fig 2.12: Influence of W via pressure when $M = 1.5$ and $\omega = 1$.

ω	S	M	$-\mathrm{Re}^{\frac{1}{2}}\, C_f$
0.3	0.1	0.9	1.45901
0.4			1.23812
0.5			0.97872
0.5	0.1	0.9	0.97873
	0.2		1.06428
	0.3		1.14991
0.3	0.1	0.8	0.43489
		0.9	1.45825
		1	1.86598

Table 2.2: Value of $-\mathrm{Re}^{\frac{1}{2}}\, C_f$ when Pr=1 and $\gamma = 0.5$

S	M	$\mathrm{Re}_s\, C_m$
0.3	0.1	0.23989
0.5		0.30109
1		0.45182
1	0.1	0.45183
	0.5	0.64390
	0.9	0.73354

Table 2.3: Value of couple $\mathrm{Re}_s\, C_m$ when $\omega = 7$.

γ	Pr	$-\theta^{'}(0)$
0	1	1.90752
0.2		1.91535
0.4		1.92210
0.2	0.9	1.90172
	1	1.91531
	1.5	1.98102

Table 2.4: Value of heat transfer rate when $\omega = 0.2$ and $S = 0.1$.

Chapter 3

Micropolar Fluid Flow over an Exponentially Stretching Curved Sheet with Variable Thermal Conductivity

In this chapter, we study the flow of micropolar fluid across an exponentially extended, curved sheet with variable thermal conductivity. Curvilinear coordinates are used in the formation of flow equations. The Cattaneo-Christov heat flux model is used for the formation of heat transfer equation. This study also takes into account the boundary layer flow along with variable thermal conductivity. The equation arising in the fluid flow is non-linear and complicated PDEs, which cannot be solved analytically. By applying suitable transformations, the PDEs are simplified into coupled and non-linear ODEs. Then we apply ND-solver command to get the desired results. The influence of parameters appearing in equations on microrotation,temperature, and velocity is also described graphically.

3.1 Mathematical Formulation

Let us consider the flow of micropolar fluid across an curved surface which is extended exponentially. The flow is steady and incompressible. Consider the curvilinear coordinate system (r, s), where r-axis is perpendicular to the direction in which fluid will flow and s-axis is in the direction of flow. Let R° denotes the radius of a circle and surface becomes flat for greater values of R°. The stretching on the surface is caused by velocity $u_w(s) = \alpha e^{\frac{s}{d}}$ (α, $d > 0$) along the s-direction where α is the initial rate of stretching and reference length is represented by d. Assuming the fluid which is electrically conducting with constant magnetic field B_0, which is directed in r-axis. Let us assume the temperature distribution $T = T(r, s)$ and velocity distribution $\mathbf{V} = [v(r, s), u(r, s)]$. The temperature of surface is T_W, where $T_W > T_\infty$ is ambient temperature of fluid. Fig 3.1 shows geometry of the fluid.

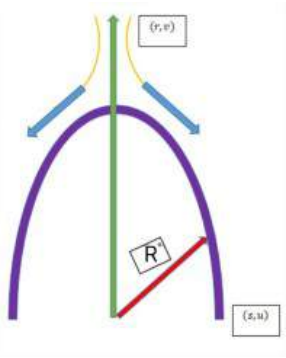

Fig 3.1 : Fluid geometry

The governing equations of the fluid based on the above assumptions are as follows:

$$\frac{\partial}{\partial r}\left((r + R^{\circ})\, v\right) + R^{\circ}\frac{\partial u}{\partial s} = 0, \tag{3.1}$$

$$\frac{\partial p}{\partial r} = \frac{\rho}{r + R^{\circ}}u^2, \tag{3.2}$$

$$\begin{aligned}\rho\left(v\frac{\partial u}{\partial r} + \frac{R^{\circ}}{R^{\circ} + r}u\frac{\partial u}{\partial s} + \frac{uv}{R^{\circ} + r}\right) &= -\frac{R^{\circ}}{R^{\circ} + r}\frac{\partial p}{\partial s} - (\mu + \overline{K})\left(\frac{\partial^2 u}{\partial r^2} + \frac{1}{R^{\circ} + r}\frac{\partial u}{\partial r} - \frac{u}{(R^{\circ} + r)^2}\right) \\ &\quad -\sigma\widetilde{B}_0^2 u - \overline{K}\frac{\partial N}{\partial r},\end{aligned} \tag{3.3}$$

$$\rho j\left(v\frac{\partial N}{\partial r}+\frac{R^{\circ}}{R^{\circ}+r}u\frac{\partial N}{\partial s}\right)=\varsigma\left(\frac{1}{R^{\circ}+r}\frac{\partial N}{\partial r}+\frac{\partial^2 N}{\partial r^2}\right)-\overline{K}\left(\frac{\partial u}{\partial r}+2N+\frac{u}{R^{\circ}+r}\right), \tag{3.4}$$

$$\left(v\frac{\partial T}{\partial r}+\frac{R^{\circ}u}{R^{\circ}+r}\frac{\partial T}{\partial s}\right)=-\frac{\nabla.[-K(T)\nabla T]}{\rho c_p}+\left(\frac{1}{R^{\circ}+r}\frac{\partial T}{\partial r}+\frac{\partial^2 T}{\partial r^2}\right)+q^*$$

$$-\lambda\begin{pmatrix} v^2\frac{\partial^2 T}{\partial r^2}+\frac{R^{\circ}u}{R^{\circ}+r}\frac{\partial u}{\partial r}\frac{\partial T}{\partial s}+\frac{R^{\circ 2}u^2}{(R^{\circ}+r)^2}\frac{\partial^2 T}{\partial s^2}+\frac{R^{\circ}u}{R^{\circ}+r}\frac{\partial v}{\partial s}\frac{\partial T}{\partial r} \\ -v\frac{\partial v}{\partial r}\frac{\partial T}{\partial r}-\frac{R^{\circ}uv}{R^{\circ}+r}\frac{\partial T}{\partial s}+\frac{2R^{\circ}uv}{R^{\circ}+r}\frac{\partial^2 T}{\partial s\partial r}+\frac{R^{\circ 2}u}{(R^{\circ}+r)^2}\frac{\partial u}{\partial r}\frac{\partial T}{\partial s} \end{pmatrix}, \tag{3.5}$$

where variable thermal conductivity in curved channel is modeled as

$$-\nabla.(-K(T)\nabla T)=\frac{\partial}{\partial r}\left(-K(T)\frac{\partial T}{\partial r}\right)-\frac{\partial}{\partial s}\left(\left(\frac{R^{\circ 2}}{(R^{\circ}+r)^2}K(T)\right)\frac{\partial T}{\partial s}\right)-\left(\frac{K(T)}{(r+R^{\circ})}\right)\frac{\partial T}{\partial r}, \tag{3.6}$$

The components of corresponding velocities is represented as (u,v) in direction (s,r) respectively. Likewise pressure is represented by p, ρ represents density, electrical conductivity is represented by σ, μ shows viscosity, $K\,(T)$ is variable thermal conductivity which also depends on temperature, $\overline{K}$ describes the vortex viscosity, T represents the temperature, N is microrotation parameter, c_p is heat capacitance, j is micro-inertia , thermal relaxation time is denoted by λ, $\varsigma=\left(\mu+\frac{\overline{K}}{2}\right)=\mu j\left(1+\frac{\beta}{2}\right)$ describes the spin gradient viscosity, where $j=\frac{2d\upsilon}{\alpha e^{\frac{s}{d}}}$.

The variable thermal conductivity is defined as linear function of temperature (ref [17])

$$K(T)=k_{\infty}[1+c(T-T_{\infty})]. \tag{3.7}$$

In above equation c is the constant which varies according to nature of fluid, k_{∞} is ambient thermal conductivity and β is micropolar parameter.

The term q^* represents heat source/sink which is non uniform and is represented by following equation

$$q^*=K\,(T)\,\frac{u_w\,(s)}{2d\nu}\left(\widehat{A}\,(T_w-T_{\infty})\,\frac{u}{u_w\,(s)}+\widehat{B}\,(T-T_{\infty})\right). \tag{3.8}$$

If the variables $\widehat{A}$, $\widehat{B}>0$, this show that heat is rising and $\widehat{A}$, $\widehat{B}<0$, this show that heat is reducing.

By using Eqs. (3.7 & 3.8) and Eq. (3.5) can be written as

$$v\frac{\partial T}{\partial r}+\frac{R^{\circ}u}{R^{\circ}+r}\frac{\partial T}{\partial s}=-\lambda\begin{pmatrix} v^2\frac{\partial^2 T}{\partial r^2}+\frac{R^{\circ}u}{R^{\circ}+r}\frac{\partial u}{\partial r}\frac{\partial T}{\partial s}+\frac{R^{\circ 2}u^2}{(R^{\circ}+r)^2}\frac{\partial^2 T}{\partial s^2}+\frac{R^{\circ}u}{R^{\circ}+r}\frac{\partial v}{\partial s}\frac{\partial T}{\partial r} \\ -v\frac{\partial v}{\partial r}\frac{\partial T}{\partial r}-\frac{R^{\circ}uv}{R^{\circ}+r}\frac{\partial T}{\partial s}+\frac{2R^{\circ}uv}{R^{\circ}+r}\frac{\partial^2 T}{\partial s\partial r}+\frac{R^{\circ 2}u}{(R^{\circ}+r)^2}\frac{\partial u}{\partial r}\frac{\partial T}{\partial s} \end{pmatrix}$$

$$-\frac{\nabla.[-K(T)\nabla T]}{\rho c_p}\left(\frac{1}{R^\circ+r}\frac{\partial T}{\partial r}+\frac{\partial^2 T}{\partial r^2}\right)-\nabla.[-K(T)\nabla T]\frac{u_w(s)}{2d\nu}\left(A\left(T_w-T_\infty\right)\frac{u}{u_w(s)}+\widehat{B}\left(T-T_\infty\right)\right). \tag{3.9}$$

The boundary condition are given as

$$\begin{aligned} u &= u_w(s), \quad v=0, \quad N=-M_r\frac{\partial u}{\partial r}, \quad T=T_w \ \text{ at } \ r=0, \\ u &\to 0, \quad \frac{\partial u}{\partial r}\to 0, \quad N\to 0, \quad T\to T_\infty \ \text{ as } \ r\to\infty, \end{aligned} \tag{3.10}$$

where $M_r\,(0\le M_r\le 1)$ shows the microrotation parameter. As microelements of the fluid cannot spin near the wall because the concentration of fluid is very high, so $M_r=0$.

Lets define the transformation

$$\eta=\sqrt{\frac{\alpha e^{\frac{s}{d}}}{2d\upsilon}}r, \tag{3.11}$$

$$\begin{aligned} u &= \alpha e^{\frac{s}{d}}f'(\eta), \quad v=\frac{-R^\circ}{R^\circ+r}\sqrt{\frac{\alpha\nu e^{\frac{s}{d}}}{2d}}\left(f(\eta)+\eta f'(\eta)\right), \quad p=\rho\alpha^2 e^{\frac{s}{d}}P(\eta), \\ N &= \alpha\sqrt{\frac{\alpha e^{\frac{s}{d}}}{2d\upsilon}}e^{\frac{s}{d}}g(\eta), \quad T=T_\infty\ (1+(\theta_w-1)\,\theta(\eta)), \quad \theta_w=\frac{T_w}{T_\infty}, \end{aligned} \tag{3.12}$$

Eqs, (3.2) to (3.9) become

$$\frac{dP}{d\eta}=\frac{1}{(\omega+\eta)}\left(\frac{df}{d\eta}\right)^2, \tag{3.13}$$

$$\begin{aligned} \frac{\omega\eta}{(\omega+\eta)}\frac{dP}{d\eta}+\frac{4\omega}{(\omega+\eta)}P &= (1+\beta)\left(\frac{d^3f}{d\eta^3}+\frac{1}{(\omega+\eta)}\frac{d^2f}{d\eta^2}-\frac{1}{(\omega+\eta)^2}\frac{df}{d\eta}\right) \\ &\quad -\frac{2\omega}{(\omega+\eta)}\left(\frac{df}{d\eta}\right)^2+\frac{\omega\eta}{(\omega+\eta)^2}\left(\frac{df}{d\eta}\right)^2+\frac{\omega}{(\omega+\eta)}f\frac{d^2f}{d\eta^2} \\ &\quad +\frac{\omega}{(\omega+\eta)^2}f\frac{df}{d\eta}-\beta\frac{dg}{d\eta}-M\frac{df}{d\eta}, \end{aligned} \tag{3.14}$$

$$\left(1+\frac{\beta}{2}\right)\left(\frac{d^2g}{d\eta^2}+\frac{1}{(\omega+\eta)}\frac{dg}{d\eta}\right)+\frac{\omega}{(\omega+\eta)}\left(f\frac{dg}{d\eta}-\frac{df}{d\eta}g\right)-\beta\left(2g+\frac{d^2f}{d\eta^2}+\frac{1}{(\omega+\eta)}\frac{df}{d\eta}\right)=0, \tag{3.15}$$

$$(1+\varepsilon\theta)\left[\frac{d^2\theta}{d\eta^2}+\frac{1}{(\omega+\eta)}\frac{d\theta}{d\eta}+\widehat{A}\frac{df}{d\eta}+\widehat{B}\theta\right]+\varepsilon\left(\frac{d\theta}{d\eta}\right)^2+\Pr\frac{\omega}{(\omega+\eta)}f\frac{d\theta}{d\eta}$$
$$+\gamma\left(\frac{\omega}{\omega+\eta}\right)^2\left[\begin{array}{c} f^2\frac{d^2\theta}{d\eta^2}+\frac{1}{(\omega+\eta)}\frac{d\theta}{d\eta}\frac{df}{d\eta}\left(f+\eta\frac{df}{d\eta}\right) \\ +\frac{d\theta}{d\eta}\left(f+\eta\frac{df}{d\eta}\right)\left(2\frac{df}{d\eta}-\eta\frac{df}{d\eta}\right)\end{array}\right]=0, \tag{3.16}$$

where

$$Pr=\frac{\mu c_p}{K\left(T\right)},\ \omega=\sqrt{\frac{\alpha e^{\frac{s}{d}}}{2dv}}R^{\circ},\ M=\frac{\sigma\widetilde{B_{\circ}}2d}{\alpha\rho},,\beta=\frac{\check{k}}{\upsilon},\gamma=\varphi\alpha,\varepsilon=c(T_w-T_\infty), \tag{3.17}$$

Pr shows the Prandtl number, ω represents the curvature, M is magnetic field, β is material parameter, thermal relaxation time is given by γ and ε shows the thermal conductivity parameter.

The non dimensional form of boundary conditions will be

$$\begin{aligned} f\left(0\right) &= 0,\quad f^{'}\left(0\right)=1,\quad g=-M_r f^{''}\left(0\right),\quad \theta^{'}\left(0\right)=-Bi\left(1-\theta\left(0\right)\right), \\ f^{'}\left(\infty\right) &\to 0,\quad f^{''}\left(\infty\right)\to 0,\quad g\left(\infty\right)\to 0,\quad \theta\left(\infty\right)\to 0, \end{aligned} \tag{3.18}$$

where

$$Bi=\frac{hd}{k_\infty},$$

h is heat transfer, Bi is Biot number, it represents the ratio of convection on surface of material to conduction inside the material. After eliminating the pressure term from Eqs. (3.13) and (3.14), we get

$$(1+\beta)\left[\frac{d^4f}{d\eta^4}+\frac{2}{(\omega+\eta)}\frac{d^3f}{d\eta^3}-\frac{1}{(\omega+\eta)^2}\frac{d^2f}{d\eta^2}+\frac{1}{(\omega+\eta)^3}\frac{df}{d\eta}\right]$$
$$-\omega\left(\frac{d^2g}{d\eta^2}+\frac{dg}{d\eta}\right)+\frac{\omega}{(\omega+\eta)}\left(f\frac{d^3f}{d\eta^3}+\frac{df}{d\eta}-f\frac{df}{d\eta}+f\frac{d^2f}{d\eta^2}\right)-M\left(\frac{df}{d\eta}+\frac{1}{(\omega+\eta)}f\right)$$
$$+\frac{1}{(\omega+\eta)}\left(\frac{df}{d\eta}\right)^2\left[\frac{-4}{(\omega+\eta)}-\frac{\omega}{(\omega+\eta)^2}+\frac{\omega}{(\omega+\eta)}-\omega\right]$$
$$+\frac{2}{(\omega+\eta)}\frac{d^2f}{d\eta^2}\left[\frac{\omega}{(\omega+\eta)}-2-\eta\omega\right]=0. \tag{3.19}$$

In field of engineering and manufacturing industries, the couple stress, skin friction are the

main application of many problems. These are given as

$$C_f = \frac{\tau_w}{\frac{1}{2}\rho\left(u_w\right)^2},\ C_s = \frac{M_w}{\mu j u_w},\ Nu = \frac{s\dot{j}_w}{k_\infty\left(T_w - T_\infty\right)}, \tag{3.20}$$

The surface heat flow, couple stress, and shear stress are shown as

$$\begin{aligned} \tau_s &= \left(\left(\mu + K\right)\left(\frac{\partial u}{\partial r} - \frac{u}{r + R^\circ}\right) + KN\right)_{r=0}, M_w = \left(\mu + \frac{K}{2}\right) j \left(\frac{\partial N}{\partial r}\right)_{r=0}, \\ q_s &= -\nabla.[-K(T)\nabla T]\left(\frac{\partial T}{\partial r}\right)_{r=0} + \frac{-16\sigma^*}{3k^*}T^3\frac{\partial T}{\partial r}, \end{aligned} \tag{3.21}$$

The above factors in non dimensional form are as follows

$$\begin{aligned} \mathrm{Re}^{\frac{1}{2}}\, C_f &= 2\left(1+\beta\right)\left(\frac{d^2 f}{d\eta^2} - \frac{1}{\beta}\frac{df}{d\eta}\right)_{\eta=0} - 2\beta M_r\left(\frac{d^2 f}{d\eta^2}\right)_{\eta=0}, \\ C_s &= \left(1 + \frac{\beta}{2}\right)\left(\frac{dg}{d\eta}\right)_{\eta=0}, \mathrm{Re}^{-\frac{1}{2}}\, Nu = -\left(1 + N_r\theta_w^3\right)\left(\frac{d\theta}{d\eta}\right)_{\eta=0}, \end{aligned} \tag{3.22}$$

where $\mathrm{Re} = \frac{u_w(s)d}{\upsilon}$ is localized Reynolds number.

3.1.1 Results and Discussion

The coupled and non-linear ODEs are now numerically simplified by the ND-Solve method. To examine the effect of magnetic force M on velocity distribution $f^{'}(\eta)$ Fig 3.2 is generated, which describes that when value of the magnetic force M rises, the velocity is reduced. The reason behind this is magnetic force produce resistance in direction of flow. Due to this, we observe that the velocity is decreased. Fig 3.3 describes the influence of microrotation parameter M_r on velocity distribution $f^{'}(\eta)$. We notice that velocity decreases when the M_r value increases. Fig 3.4 describes the influence of material factor β on the velocity distribution $f^{'}(\eta)$, which shows that by increasing β, the velocity also increases. Because β is inversely proportional to viscosity, as viscosity decreases the thickness of boundary layer also decreases. From Fig 3.5, we observe that the influence of curvature ω on velocity $f^{'}(\eta)$. We notice that by raising the curvature values the velocity also grows because the radius of the exponential surface expands, which cause an increase in velocity. To show the influence of magnetic force on microrotation. Fig 3.6

is generated which shows that when the values of M enhances the microrotation distribution $g(\eta)$ decreases due to the Lorentz force caused by magnetic field which produces disturbance in the flow. Fig 3.7 depicts the effect of microrotation parameter M_r on $g(\eta)$. We observe that when values of M_r increases the microrotation distribution also rises. In Fig 3.8, we have seen the effect of material parameter β on microrotation which describes as β increases $g(\eta)$ also increases. e reason for this is that boundary layer thickness decreases as viscosity decreases because β and viscosity are inversely proportional. Fig 3.9 describes the influence of biot number on temperature $\theta(\eta)$. We see that temperature rises when values of Bi rises. Fig 3.10 describes how the Prandtl number effects temperature. The temperature decreases as we enhances Pr values. Basically Pr is ratio between thermal diffusivity and momentum diffusivity because the temperature and the boundary layer thickness both reduce when Pr increases. Fig 3.11, 3.12 show how increase in $\widehat{A}$, $\widehat{B}$ values effects temperature $\theta(\eta)$. We observe temperature rises due to the presence of irregular heat factors. Fig 3.13 is plotted to show the impact of curvature ω of temperature $\theta(\eta)$, the temperature decreases when curvature values rises. Because the radius of the exponential surface increases then the temperature reduces. We notice the effect of thermal conductivity ε on temperature in Fig 3.14. When thermal conductivity increases temperature also rises.

Tables 3.1,3.2 and 3.3 are calculated to analyze the numerical results of skin friction, couple stress and rate of heat transfer for various values of M, ω and β. From Table 3.1, it is shown that the value of skin friction reduces by increasing the value of curvature, and if we rise the value of M and β skin friction value also increases. It is observed from Table 3.2 that couple stress coefficient increases when value of M and β rises, while keeping the value of ω constant. Table 3.3 illustrates that rate at which heat transfer increases by rising the value of Pr and γ. Table 3.4 shows the comparison of skin friction of present work with published work Alqahtani[5].

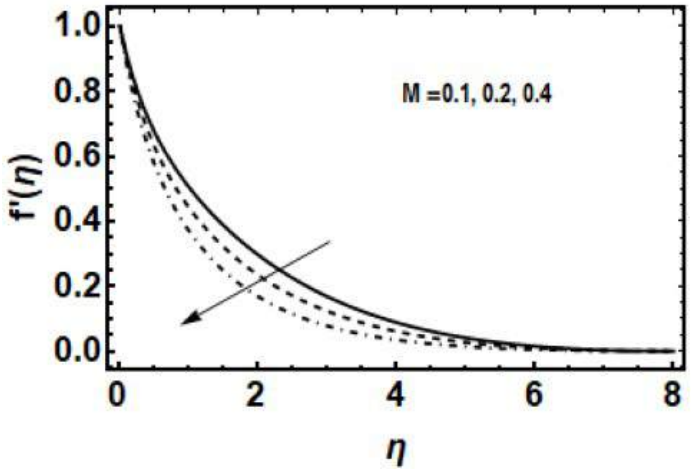

Fig 3.2: Influence of M via velocity when $\omega = 1.5$ and $M_r = 0.1$

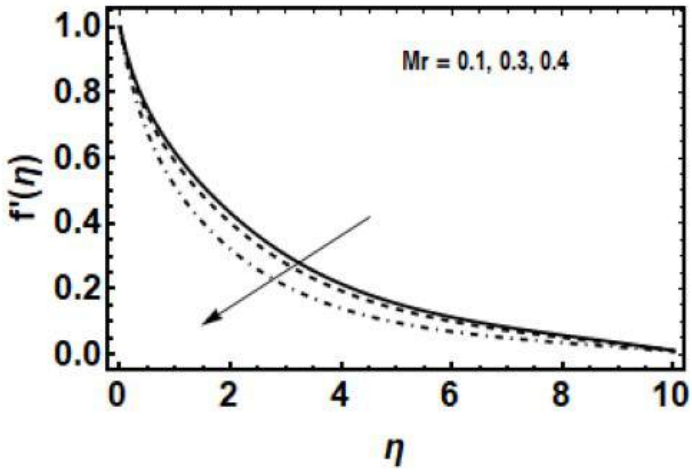

Fig 3.3: Influence of M_r via velocity $\omega = 1.4$ and $M = 0.4$.

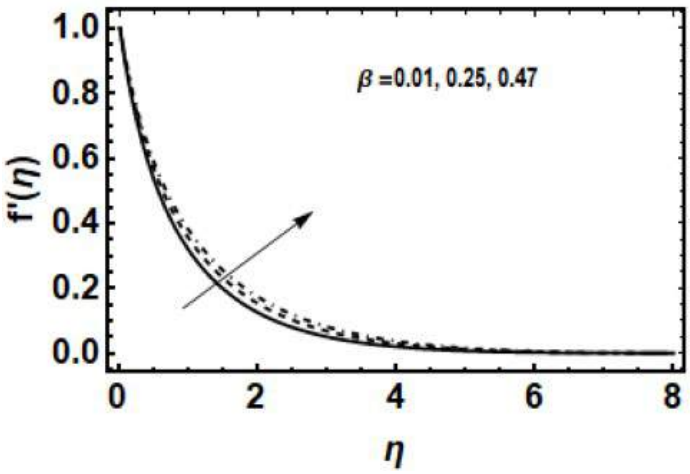

Fig 3.4: Influence of β via velocity when $\omega = 1.5$ and $M = 0.3$.

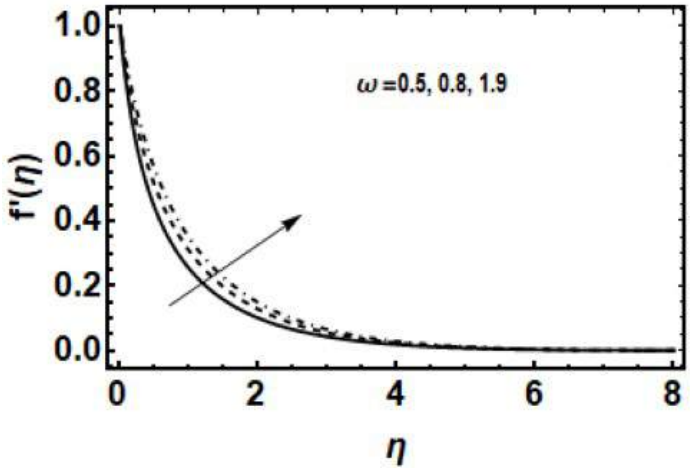

Fig 3.5: Influence of curvature via velocity when $\beta = 0.2$ and $M = 0.5$.

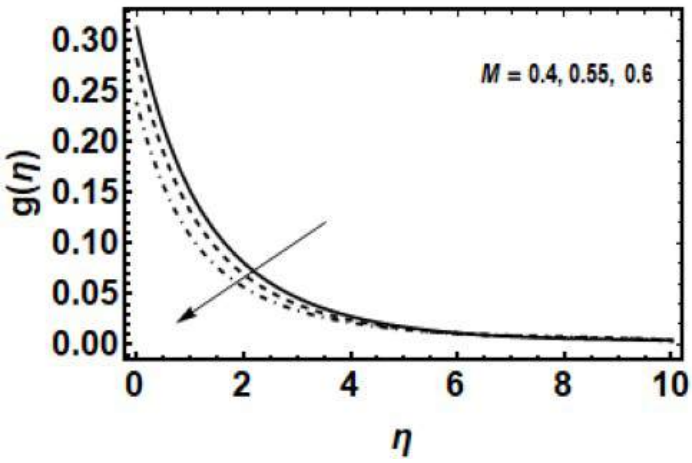

Fig 3.6: Influence of M via microrotation when $M_r = 0.3$ and $\beta = 0.2$.

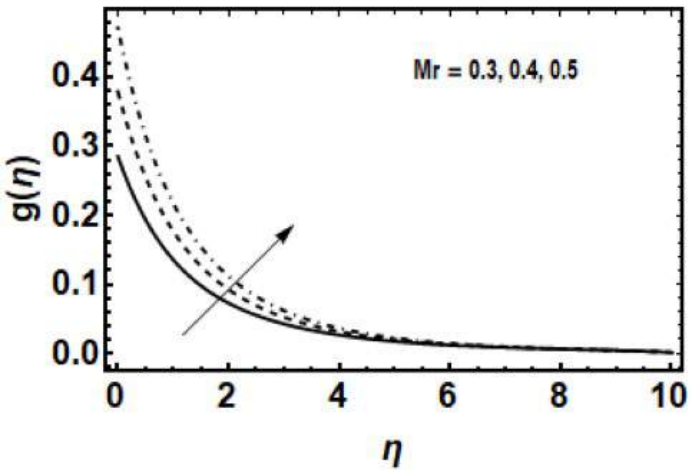

Fig 3.7: Influence of M_r via microrotation when $M = 0.4$ and $\beta = 0.2$.

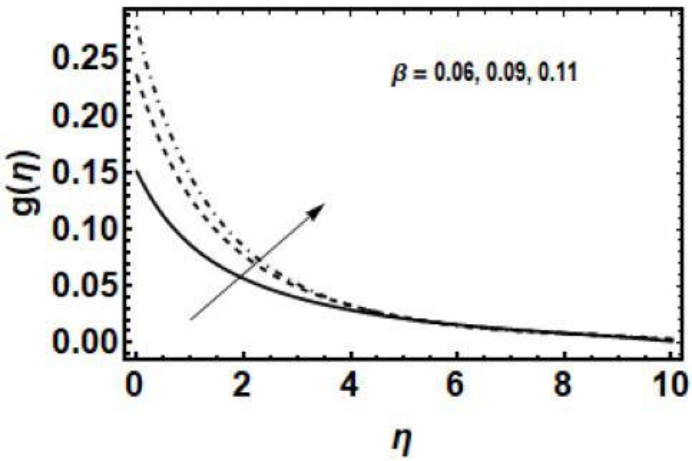

Fig 3.8: Influence of β via micro rotation when $M = 0.7$ and $M_r = 0.3$.

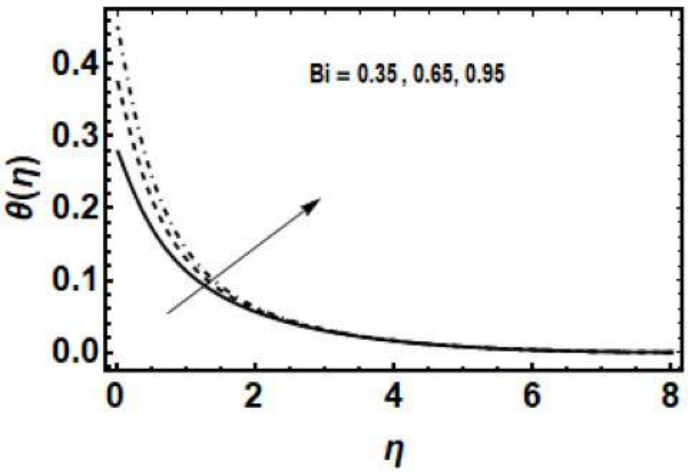

Fig 3.9: Influence of Bi via temperature when $\omega = 1.5$ and $M = 0.5$.

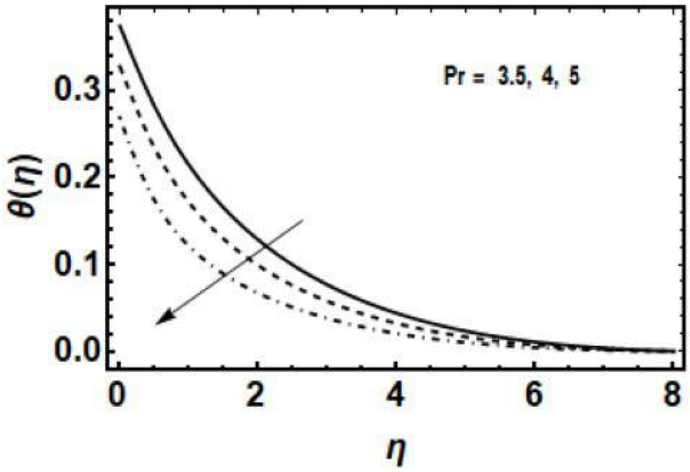

Fig 3.10: Influence of Pr via temperature when $\omega = 1.5$ and $M = 0.2$.

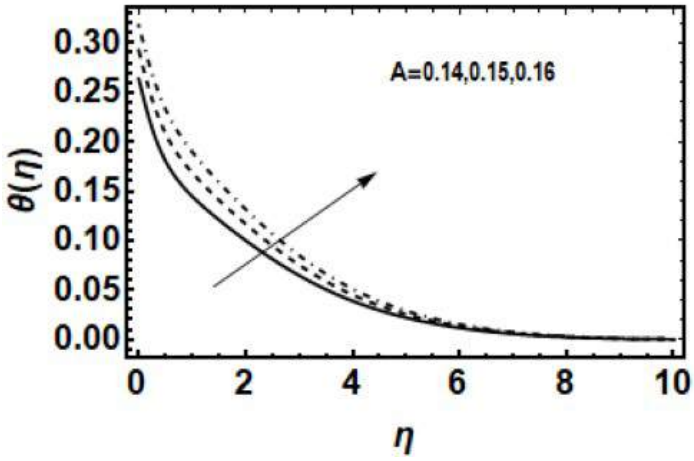

Fig 3.11: Influence of $\widehat{A}$ via temperature when $\omega = 1.5$ and $M = 0.2$.

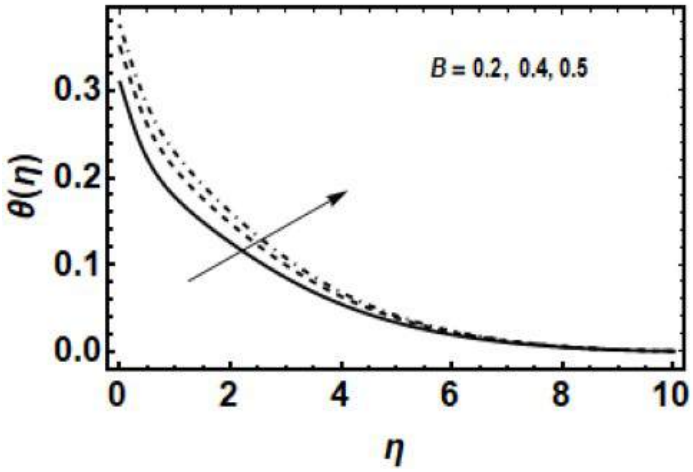

Fig 3.12: Influence of $\widehat{B}$ via temperature when $\omega = 1.5$ and $M = 0.2$.

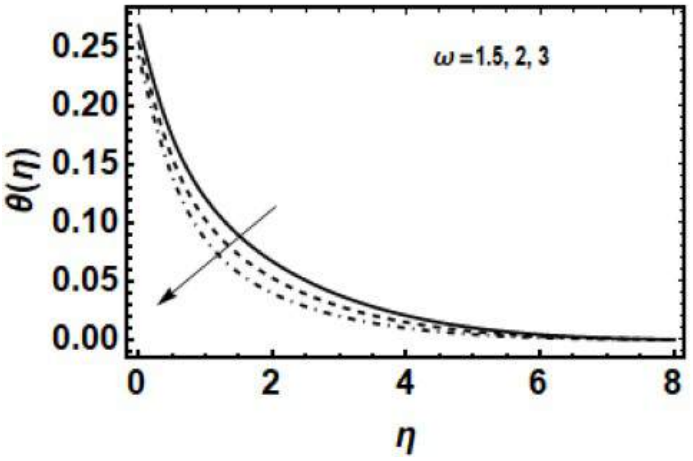

Fig 3.13: Influence of curvature ω via temperature when $M = 0.2$ and $\mathrm{Pr} = 5$.

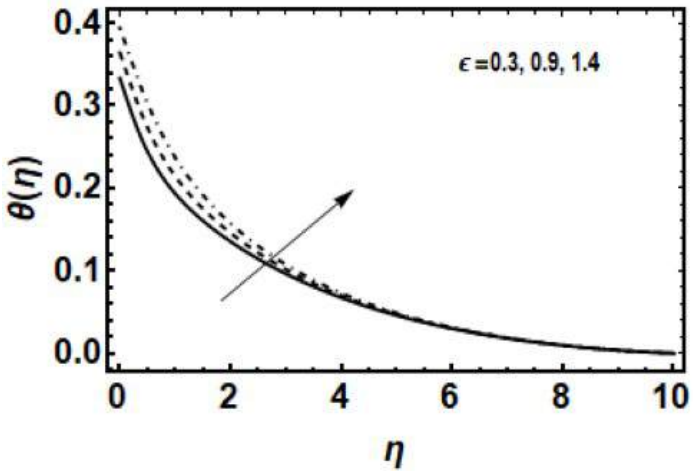

Fig 3.14: Influence of thermal conductivity via temperature when $M = 0.3$ and $\mathrm{Pr} = 5$.

ω	β	M	$-\mathrm{Re}^{\frac{1}{2}} C_f$
1.5	0.6	0.9	0.74651
1.8			0.65943
2.5			0.58972
1.8	0.5	0.5	0.45853
	0.6		0.63018
	0.9		0.78699
1.8	0.6	0.9	0.65943
		1.1	0.70581
		1.6	0.73219

Table 3.1: Value of $-\mathrm{Re}^{\frac{1}{2}} C_f$ when Pr=3 and $\gamma = 0.7$

β	M	$\mathrm{Re}_s\, C_m$
0.4	0.5	0.01343
0.6		0.01368
1.2		0.01881
0.9	0.7	0.01767
	0.85	0.01838
	0.9	0.01904

Table 3.2: Value of couple $\mathrm{Re}_s\, C_m$ when $\omega = 1$.

γ	Pr	$-\theta^{'}(0)$
0.1	3	0.13424
0.15		0.14618
0.2		0.15352
0.1	1	0.31660
	1.5	0.48672
	2	0.57226

Table 3.3: Value of heat transfer rate when $\omega = 1$ and $\beta = 0$.

β	Pr	$-\theta^{'}(0)$
0.5	1.52075	1.52054
1	1.45782	1.45745
1.5	1.42466	1.42479
2	1.41392	1.41368
2.5	1.30860	1.30852
3	1.30558	1.30565

Table 3.4: Comparison of skin friction of present work with published work.

3.2 Conclusion

The main objective of this chapter is to examine the rate at which heat will transfer in a magnetohydrodynamic flow of micropolar fluid across an exponentially stretched curved surface. The flow is steady and incompressible. The key points are:

· By increasing MHD the velocity and microrotation distribution decreases.

· Temperature reduces by enhancing Prandtl number.

· By increasing the material parameter, velocity decreases and microrotation increases.

· The velocity and microrotation curves both increases when material parameter rises.

· By rising the curvature values, the velocity profile increases and the temperature decreases.

Bibliography

[1] Muhammad, T., Rafique, K., Asma, M., & Alghamdi, M. (2020). Darcy–Forchheimer flow over an exponentially stretching curved surface with Cattaneo–Christov double diffusion. Physica A: Statistical Mechanics and its Applications, 556, 123968.

[2] Kempannagari, A. K., Buruju, R. R., Naramgari, S., & Vangala, S. (2020). Effect of Joule heating on MHD non-Newtonian fluid flow past an exponentially stretching curved surface. Heat Transfer, 49(6), 3575-3592.

[3] Shi, Q. H., Shabbir, T., Mushtaq, M., Khan, M. I., Shah, Z., & Kumam, P. (2021). Modelling and numerical computation for flow of micropolar fluid towards an exponential curved surface: a Keller box method. Scientific Reports, 11(1), 16351.

[4] Kumar, K. A., Sugunamma, V., Sandeep, N., & Sivaiah, S. (2020, June). Physical aspects on MHD micropolar fluid flow past an exponentially stretching curved surface. In Defect and Diffusion Forum (Vol. 401, pp. 79-91). Trans Tech Publications Ltd.

[5] Alqahtani, A. M., Khan, W., Alhabeeb, S. A., & Khalifa, H. A. E. W. (2023). Stability of magnetohydrodynamics free convective micropolar thermal liquid movement over an exponentially extended curved surface. Heliyon, 9(11).

[6] Hafeez, A., Khan, M., & Ahmed, J. (2020). Flow of Oldroyd-B fluid over a rotating disk with Cattaneo–Christov theory for heat and mass fluxes. Computer methods and programs in biomedicine, 191, 105374.

[7] Khan, M. (2017). On Cattaneo–Christov heat flux model for Carreau fluid flow over a slendering sheet. Results in Physics, 7, 310-319.

[8] Rehman, S., Muhammad, N., Alshehri, M., Alkarni, S., Eldin, S. M., & Shah, N. A. (2023). Analysis of a viscoelastic fluid flow with Cattaneo–Christov heat flux and Soret–Dufour effects. Case Studies in Thermal Engineering, 49, 103223.

[9] Nadeem, S., Ahmad, S., & Muhammad, N. (2017). Cattaneo-Christov flux in the flow of a viscoelastic fluid in the presence of Newtonian heating. Journal of Molecular liquids, 237, 180-184.

[10] Khan, M. (2017). On Cattaneo–Christov heat flux model for Carreau fluid flow over a slendering sheet. Results in Physics, 7, 310-319.

[11] Straughan, B. (2010). Thermal convection with the Cattaneo–Christov model. International Journal of Heat and Mass Transfer, 53(1-3), 95-98.

[12] Straughan, B. (2010). Acoustic waves in a Cattaneo–Christov gas. Physics Letters A, 374(26), 2667-2669.

[13] Angeles, F., Málaga, C., & Plaza, R. G. (2020). Strict dissipativity of Cattaneo–Christov systems for compressible fluid flow. Journal of Physics A: Mathematical and Theoretical, 53(6), 065701.

[14] Usman M., Hamid, M., Zubair, T., Haq, R. U., & Wang, W. (2018). Cu-Al2O3/Water hybrid nanofluid through a permeable surface in the presence of nonlinear radiation and variable thermal conductivity via LSM. International Journal of Heat and Mass Transfer, 126, 1347-1356.

[15] Gbadeyan, J. A., Titiloye, E. O., & Adeosun, A. T. (2020). Effect of variable thermal conductivity and viscosity on Casson nanofluid flow with convective heating and velocity slip. Heliyon, 6(1).

[16] Mustafa, M., Hayat, T., & Alsaedi, A. (2017). Rotating flow of Maxwell fluid with variable thermal conductivity: an application to non-Fourier heat flux theory. International Journal of Heat and Mass Transfer, 106, 142-148.

[17] Mahmoud, M. A. (2007). Thermal radiation effects on MHD flow of a micropolar fluid over a stretching surface with variable thermal conductivity. Physica A: Statistical Mechanics and its Applications, 375(2), 401-410.

[18] Rafaqat, R., Khan, A. A., & Zaman, A. (2022). Unsteady radiative–convective flow of a compressible fluid: a numerical approach. Canadian Journal of Physics, 101(5), 203-210.